



A line integral-based method to partition climate and catchment effects on runoff

Mingguo Zheng^{1, 2*}

¹ Guangdong Key Laboratory of Agricultural Environment Pollution Integrated Control, Guangdong Institute of Eco-environment Science & Technology, Guangzhou 510650, China

² Key Laboratory of Water Cycle and Related Land Surface Processes, Institute of Geographic Sciences & Natural Resources Research, Chinese Academic of Sciences, Beijing 100101, China

Correspondence: Mingguo Zheng (mgzheng@soil.gd.cn)

Abstract

It is a common task to partition synergistic impacts of a number of drivers in the environmental sciences. However, there is no mathematically precise solution to the partition. Here I presented a line integral-based method, which concerns about the sensitivity to the drivers throughout their evolutionary path so as to ensure a precise partition. The method reveals that the partition depends on both the change magnitude and pathway (timing of change), and not on the magnitude alone unless for a linear system. To illustrate the method, I used the Budyko framework to partition the effects on the temporal change in runoff of climatic and catchment conditions for 21 catchments from Australia and China. The method reduced to the decomposition method when assumed a path along which climate change occurs first followed by an abrupt change in catchment properties. The method re-defines the widely-used concept of sensitivity at a point as the path-averaged sensitivity. The total differential and the complementary methods simply concern about the sensitivity at the initial or/and the terminal state, so that they cannot give precise results. The path-average sensitivity of water yield to climate conditions was found to be stable over time. Space-wise, moreover, it can be readily predicted even in the absence of streamflow observations, whereby facilitates evaluation of future climate effects on streamflow. As a mathematically accurate solution, the method provides a generic tool to conduct the quantitative attribution analyses.

Keywords: Runoff; Climate change; Human activities; Attribution analysis; Budyko

1 Introduction

It is often needed to quantify the relative roles of a few drivers to the observed changes of interest in the environmental sciences. In the hydrology community, diagnosing the relative contributions of climate change and human activities to runoff is of great relevance to the researchers and managers as both climate change and human activities have pose global-scale impact on hydrologic cycle and water resources (Barnett *et al.*, 2008; Xu *et al.*, 2014; Wang and Hejazi, 2001). To date, unfortunately, the quantitative attribution analysis of the runoff changes remains a challenge (Wang and Hejazi, 2001; Berghuijs and Woods, 2016; Zhang *et al.*, 2016); this is to a considerable degree due to a



39 lack of a mathematically precise method to decouple synergistic and often confounding impacts of
40 climate change and human activities.

41 Numerous studies have detected the long term variability in runoff and attempted to partition the
42 effects of climate change and human activities by means of various methods (Dey and Mishra, 2017).
43 Among them are the paired-catchments method and the hydrological modeling method. The paired-
44 catchment method is believed to be able to filter the effect of climatic variability and thus isolate the
45 runoff change induced by vegetation changes (Brown *et al.*, 2005). However, the method is
46 capital intensive. Particularly, it generally involves small catchments and is challenged when
47 extrapolating to large catchments (Zhang *et al.*, 2011). The physical-based hydrological models often
48 suffer from limitations including high data requirement, labor-intensive calibration and validation
49 processes, and inherent uncertainty and interdependence in parameter estimations (Binley *et al.*, 1991;
50 Wang *et al.*, 2013; Liang *et al.*, 2015). Interest then turns to the conceptual models over recent years,
51 such as the Budyko-type equations (see Section 2.1).

52 Within the Budyko framework, a large number of studies (Roderick and Farquhar, 2011; Zhang
53 *et al.*, 2016) have used the total differential as a proxy for the runoff change and further evaluated
54 hydrological responses to climate change and human activities (hereafter called the total differential
55 method). The total differential, however, is essentially a first-order approximation of the observed
56 change. It has been shown that the approximation has caused an error of the climate impact on runoff
57 ranging from 0 to 20 mm (or -118 to 174%) over China (Yang *et al.*, 2014). The total differential
58 method directly used the partial derivatives of runoff to estimate the sensitivities of runoff to climate
59 and catchment conditions. Most studies applied the forward approximation of the runoff change, *i.e.*,
60 using the sensitivities at the initial state while calculation (e.g. Roderick and Farquhar, 2011). The
61 elasticity method proposed by Schaake (1990) is also based on the total differential expression
62 (Sankarasubramanian *et al.*, 2001; Zheng *et al.*, 2009). The method uses the “elasticity” concept to
63 assess the climate sensitivity of runoff. The elasticity coefficients, however, have been estimated in an
64 empirical way and is not physically sound (Roderick and Farquhar, 2011; Liang *et al.*, 2015).

65 The so-called decomposition method developed by Wang and Hejazi (2011) has also been
66 widely used. The method assumes that climate changes drive a shift along a Budyko curve and then
67 human interferences cause a vertical shift from the Budyko curve to another. Under this assumption, the
68 method directly extrapolates the Budyko models calibrated using observations of the reference period,
69 in which human impacts remain minimal, to determine the human-induced changes in runoff occurred
70 during the evaluation period.

71 Recently, Zhou *et al.* (2016) established a Budyko complementary relationship for runoff and
72 applied it to partitioning the climate and catchment effects. Superior to the total differential method, the
73 method culminates with yielding a no-residual partition. Nevertheless, the method depends on a given
74 weighted factor, which is determined in an empirical but not a precise way. Furthermore, Zhou *et al.*
75 (2016) argued that the partition is not unique in the Budyko framework as the path of the climate and
76 catchment changes cannot be uniquely identified.

77 Actually, a precise partition remains difficult even given a precise mathematical model. This
78 can be illustrated by using a precise hydrology model $R = f(x, y)$, where R represents runoff, and x and y
79 climate factors and catchment characteristics respectively. We assumed that R changes by ΔR when x
80 changes by Δx and y by Δy , *i.e.* $\Delta R = f(x + \Delta x, y + \Delta y) - f(x, y)$. To determine the effect of x on ΔR ,



81 *i.e.* ΔR_x , a common practice is to assume that y remains constant when x changes by Δx . We thus get:
82 $\Delta R_x = f(x + \Delta x, y) - f(x, y)$. Similarly, we can get: $\Delta R_y = f(x, y + \Delta y) - f(x, y)$. Although the
83 derivation seems quite reasonable, it is problematic as the sum of ΔR_x and ΔR_y is not equal to ΔR .
84 Further examination shows that a variable's effect on R should differ depending on the changing path.
85 For example, $\Delta R_x = f(x + \Delta x, y) - f(x, y)$ and $\Delta R_y = f(x + \Delta x, y + \Delta y) - f(x + \Delta x, y)$ if x changes first
86 and y subsequently (Note that the sum of ΔR_x and ΔR_y equals ΔR now). If y changes first and x
87 subsequently, in contrast, the expressions become: $\Delta R_x = f(x + \Delta x, y + \Delta y) - f(x, y + \Delta y)$ and
88 $\Delta R_y = f(x, y + \Delta y) - f(x, y)$. In case of x and y changing simultaneously, unfortunately,
89 current literature seems not to provide a mathematically precise solution.

90 The aims of this work are to propose a new and mathematically precise method to conduct
91 quantitative attribution to the drivers. The method is based on the line integer (called the LI method
92 hereafter) and takes account of the sensitivity throughout the evolutionary path of the drivers, thus
93 revising the widely-used concept of sensitivity at a point as the path-averaged sensitivity. To present
94 and evaluate the method, I decomposed the relative influences of climate and catchment conditions on
95 runoff within the Budyko framework using data from 21 catchments from Australia and China. I also
96 examined the spatio-temporal variability of the path-averaged sensitivities of runoff to climatic and
97 catchment conditions and assessed their spatio-temporal predictability.

98

99 2 Methodology

100 2.1 The Budyko Framework and the MCY equation

101 Budyko (1974) argued that the mean annual evapotranspiration (E) is largely determined by
102 water and energy balance of a catchment. Using precipitation (P) and potential evapotranspiration (E_0)
103 as proxies for water and energy availabilities respectively, the Budyko framework
104 relates evapotranspiration losses to the aridity index defined as the ratio of E_0 over P . The Budyko
105 framework has gained wide acceptance in the hydrology community (Berghuijs and Woods, 2016;
106 Sposito, 2017). Over past decades, a number of equations have been developed to describe the
107 framework. Among them, the Mezentsev-Choudhury-Yang's equation (Mezentsev, 1955; Choudhury,
108 1999; Yang *et al.*, 2008) (Called the MCY equation hereafter) has been widely accepted and was used
109 here:

$$110 \quad \frac{E}{P} = \frac{E_0/P}{(1 + (E_0/P)^n)^{1/n}} \quad (1)$$

111 where $n \in (0, \infty)$ is an integration constant that is dimensionless, and represents catchment properties.
112 Eq. (3) requires a relative long time scale whereby the water storage of a catchment is negligible and the
113 water balance equation reduces to be $R = P - E$, where R denotes mean annual runoff. Here I adopted a
114 "tuned" n value that can get exact agreement between the calculated E by Eq. (1) and that actually
115 encountered ($= P - R$).

116 The partial differentials of R with respect to P , E_0 , and n are given as:



$$117 \quad \frac{\partial R}{\partial P} = R_P(P, E_0, n) = 1 - \frac{E_0^{n+1}}{(P^n + E_0^n)^{1/n}} \quad (2a)$$

$$118 \quad \frac{\partial R}{\partial E_0} = R_{E_0}(P, E_0, n) = -\frac{P^{n+1}}{(P^n + E_0^n)^{1/n}} \quad (2b)$$

$$119 \quad \frac{\partial R}{\partial n} = R_n(P, E_0, n) = \frac{-E_0 P n^{-1}}{(P^n + E_0^n)^{1/n}} \left[\frac{\ln(P^n + E_0^n)}{n} - \frac{P^n \ln P + E_0^n \ln E_0}{P^n + E_0^n} \right] \quad (2c)$$

120 2.2 The theory of the line integral-based method

121 To present the LI method, we start by considering an example of a two-variable function $z = f(x,$
 122 $y)$, which has continuous partial derivatives $\partial z / \partial x = f_x(x, y)$ and $\partial z / \partial y = f_y(x, y)$. Suppose that x and y
 123 varies along a smooth curve L (e.g. AC in Fig. 1) from the initial state (x_0, y_0) to the terminal state $(x_N,$
 124 $y_N)$, and z co-varies from z_0 to z_N . Let $\Delta z = z_N - z_0$, $\Delta x = x_N - x_0$, and $\Delta y = y_N - y_0$. Our goal is to seek
 125 for a mathematical solution to quantify the effects of Δx and Δy on Δz , i.e. Δz_x and Δz_y . Δz_x and Δz_y
 126 should be subject to the constraint $\Delta z_x + \Delta z_y = \Delta z$.

127 As shown in Fig. 1, points $M_1(x_1, y_1), \dots, M_{N-1}(x_{N-1}, y_{N-1})$ partition L into N distinct segments. Let
 128 $\Delta x_i = x_{i+1} - x_i$, $\Delta y_i = y_{i+1} - y_i$, and $\Delta z_i = z_{i+1} - z_i$. For each segment, Δz_i can be approximated as the
 129 total differential dz_i : $\Delta z_i \approx dz_i = f_x(x_i, y_i)\Delta x_i + f_y(x_i, y_i)\Delta y_i$. We then have:

$$130 \quad \Delta z = \sum_{i=1}^N \Delta z_i \approx \sum_{i=1}^N f_x(x_i, y_i)\Delta x_i + \sum_{i=1}^N f_y(x_i, y_i)\Delta y_i. \text{ We thus obtain an approximation of } \Delta z_x \text{ and } \Delta z_y :$$

$$131 \quad \Delta z_x \approx \sum_{i=1}^N f_x(x_i, y_i)\Delta x_i \text{ and } \Delta z_y \approx \sum_{i=1}^N f_y(x_i, y_i)\Delta y_i. \text{ Define } \tau \text{ as the maximum length among the } N \text{ segments.}$$

132 The smaller the value of τ , the closer to Δz_i the value of dz_i , and then the better the approximations are.
 133 The approximations would become exact in the limit $\tau \rightarrow 0$. Taking the limit $\tau \rightarrow 0$ then turns sum into
 134 integrals and gives a precise expression (it is an informal derivation and please see Appendix A for a

$$135 \text{ formal one): } \Delta z = \lim_{\tau \rightarrow 0} \sum_{i=1}^N f_x(x_i, y_i)\Delta x_i + \lim_{\tau \rightarrow 0} \sum_{i=1}^N f_y(x_i, y_i)\Delta y_i = \int_L f_x(x, y)dx + \int_L f_y(x, y)dy, \text{ where}$$

$$136 \quad \int_L f_x(x, y)dx = \lim_{\tau \rightarrow 0} \sum_{i=1}^N f_x(x_i, y_i)\Delta x_i \text{ and } \int_L f_y(x, y)dy = \lim_{\tau \rightarrow 0} \sum_{i=1}^N f_y(x_i, y_i)\Delta y_i \text{ denote the line integral of } f_x \text{ and } f_y$$

137 along L (termed integral path) with respect to x and y , respectively. $\int_L f_x(x, y)dx$ and $\int_L f_y(x, y)dy$ exist
 138 provided that f_x and f_y are continuous along L . We thus obtain a precise evaluation of Δz_x and Δz_y :

$$139 \quad \Delta z_x = \int_L f_x(x, y)dx \quad (3a)$$

$$140 \quad \Delta z_y = \int_L f_y(x, y)dy. \quad (3b)$$

141 Mathematically, the sum of Δz_x and Δz_y persistently equals Δz , independent of the curve L
 142 (Appendix B). If $f(x, y)$ is linear, then f_x and f_y are constant. Define $C_x = f_x(x, y)$ and $C_y = f_y(x, y)$, we
 143 have $\Delta z_x = C_x \Delta x$ and $\Delta z_y = C_y \Delta x$. Δz_x and Δz_y are thus independent of L . If $f(x, y)$ is non-linear, in contrast,



144 both Δz_x and Δz_y varies with L , as was exemplified in Appendix C. Hence, the initial and the terminal
 145 states, together with the path connecting them, determines Δz_x and Δz_y unless $f(x, y)$ is linear.

146 The mathematical derivation above applies to a three-variable function as well. By doing the line
 147 integrals for the MCY equation, we obtain the desired results:

148
$$\Delta R_P = \int_L \frac{\partial R}{\partial P} dP \quad (4a)$$

149
$$\Delta R_{E_0} = \int_L \frac{\partial R}{\partial E_0} dE_0 \quad (4b)$$

150
$$\Delta R_n = \int_L \frac{\partial R}{\partial n} dn \quad (4c)$$

151 where ΔR_P , ΔR_{E_0} , and ΔR_n denotes the effects on runoff change of P , E_0 , and n , respectively. The sum of
 152 ΔR_P and ΔR_{E_0} represents the effect of climate change, and ΔR_n are often related to human activities
 153 although it probably includes the effects of other factors, such as climate seasonality (Roderick and
 154 Farquhar, 2011; Berghuijs and Woods, 2016). L denotes a three-dimensional curve along which climate
 155 and catchment changes have occurred. I approximated L as a union of a series of line segments. ΔR_P ,
 156 ΔR_{E_0} , and ΔR_n were finally figured out by summing up the integrals along each of the line segments (see
 157 Section 2.3).

158 **2.3 Using the LI method to determine ΔR_P , ΔR_{E_0} , and ΔR_n within the Budyko Framework**

159 **1) Determining ΔR_P , ΔR_{E_0} , and ΔR_n assuming a linear integral path**

160 Given two consecutive periods and assumed that the catchment state has evolved from $(P_1, E_{01},$
 161 $n_1)$ to (P_2, E_{02}, n_2) along a straight line L . Let $\Delta P = P_2 - P_1$, $\Delta E_0 = E_{02} - E_{01}$, and $\Delta n = n_2 - n_1$, then the
 162 line L is given by the parametric equations: $P = \Delta Pt + P_1$, $E_0 = \Delta E_0 t + E_{01}$, $n = \Delta n t + n_1$, $t \in [0, 1]$. Given
 163 the equations, Eq. (2) becomes a one-variable function of t , i.e., $\partial R / \partial P = R_P(t)$, $\partial R / \partial E_0 = R_{E_0}(t)$, and
 164 $\partial R / \partial n = R_n(t)$. Then, ΔR_P , ΔR_{E_0} , and ΔR_n can be evaluated as:

165
$$\Delta R_P = \int_L \frac{\partial R}{\partial P} dP = \int_0^1 R_P(t) d(\Delta Pt + P_1) = \Delta P \int_0^1 R_P(t) dt \quad (5a)$$

166
$$\Delta R_{E_0} = \int_L \frac{\partial R}{\partial E_0} dE_0 = \int_0^1 R_{E_0}(t) d(\Delta E_0 t + E_{01}) = \Delta E_0 \int_0^1 R_{E_0}(t) dt \quad (5b)$$

167
$$\Delta R_n = \int_L \frac{\partial R}{\partial n} dn = \int_0^1 R_n(t) d(\Delta n t + n_1) = \Delta n \int_0^1 R_n(t) dt \quad (5c)$$

168 Unfortunately, I cannot figure out the antiderivatives of $R_P(t)$, $R_{E_0}(t)$, and $R_n(t)$ and have to make
 169 approximate calculations. I divided the $t \in [0, 1]$ interval into 1000 subintervals of the same width,
 170 thereby setting dt identically equal to 0.001. I then calculated $R_P(t)dt$, $R_{E_0}(t)dt$, and $R_n(t)dt$ for each
 171 subinterval. Let $t_i = 0.001i$, $i \in [0, 999]$ and is integer-valued, ΔR_P , ΔR_{E_0} , and ΔR_n was approximated as:

172
$$\Delta R_P \approx 0.001 \Delta P \sum_{i=0}^{999} R_P(t_i) \quad (6a)$$

173
$$\Delta R_{E_0} \approx 0.001 \Delta E_0 \sum_{i=0}^{999} R_{E_0}(t_i) \quad (6b)$$



$$\Delta R_n \approx 0.001 \Delta n \sum_{i=0}^{999} R_n(t_i) \quad (6c)$$

2) Dividing the evaluation period into a number of subperiods

I first determine a change point and divide the whole observation period into the reference and evaluation periods. To determine the integral path, the evaluation period is further divided into a number of subperiods. The Budyko framework assumes a steady state condition of a catchment and therefore requires no change in soil water storage. Over a time period of 5-10 years, it is reasonable to assume that changes in soil water storage are sufficiently small (Zhang *et al.*, 2001). Here I divided the evaluation period into a number of 7-year subperiods with the exception for the last one, which varied from 7 to 13 years in length depending on the length of the evaluation period.

3) Determining ΔR_P , ΔR_{E_0} , and ΔR_n by approximating the integral path as a series of line segments

For a short period, the integral path L can be considered as linear, which implies a uniform change over time. If the change is not uniform over a given long period, the integral path L can be fitted using a number of line segments. Given a reference period and an evaluation period comprising N subperiods, I assumed that the catchment state evolved from $(P_0, E_{00}, n_0), \dots, (P_i, E_{0i}, n_i), \dots$, to (P_N, E_{0N}, n_N) , where the subscript "0" denotes the reference period, and "i" and "N" denotes the i th and the last subperiods of the evaluation period, respectively. I used a series of line segments L_1, L_2, \dots, L_N to approximate the integral path L , where the initial point of L_{i+1} is the terminal point of L_i , and L_i connects points $(P_{i-1}, E_{0,i-1}, n_{i-1})$ with (P_i, E_{0i}, n_i) and L_1 connects (P_0, E_{00}, n_0) with (P_1, E_{01}, n_1) . Then ΔR_P , ΔR_{E_0} , and ΔR_n are determined as the sum of the integrals along each of the line segments, which was calculated using Eq. (6).

2.4 The total-differential, decomposition and complementary methods

To evaluate the LI method, I compared it with the decomposition method, the total differential method, and the complementary method. The total differential method approximated ΔR as dR :

$$\Delta R \approx dR = \frac{\partial R}{\partial P} \Delta P + \frac{\partial R}{\partial E_0} \Delta E_0 + \frac{\partial R}{\partial n} \Delta n = \lambda_P \Delta P + \lambda_{E_0} \Delta E_0 + \lambda_n \Delta n \quad (7)$$

where $\lambda_P = \partial R / \partial P$, $\lambda_{E_0} = \partial R / \partial E_0$, and $\lambda_n = \partial R / \partial n$, representing the sensitivity coefficient of R with respect to P , E_0 , and n , respectively. Within the total differential method, $\Delta R_P = \lambda_P \Delta P$, $\Delta R_{E_0} = \lambda_{E_0} \Delta E_0$, and $\Delta R_n = \lambda_n \Delta n$. I used a forward approximation, *i.e.* substituting the observed mean annual values of the reference period into Eq. (2), to estimate λ_P , λ_{E_0} , and λ_n , as did in most studies (Roderick and Farquhar, 2011; Yang and Yang, 2011; Sun *et al.*, 2014).

The decomposition method (Wang and Hejazi, 2011) calculated ΔR_n as follows:

$$\Delta R_n = R_2 - R'_2 = (P_2 - E_2) - (P_2 - E'_2) = E'_2 - E_2 \quad (8)$$

where R_2 , P_2 , and E_2 represents the mean annual runoff, precipitation and evapotranspiration of the evaluation period; and R'_2 and E'_2 represents the mean annual runoff and evapotranspiration respectively, given the climate conditions of the evaluation period and the catchment conditions of the reference period. Both E_2 and E'_2 were calculated by Eq. (1), but using n values of the evaluation period and the reference period respectively.



210 The complementary method (Zhou *et al.*, 2016) uses a linear combination of the complementary
 211 relationship for runoff to determine ΔR_P , ΔR_{E_0} , and ΔR_n :

$$212 \quad \Delta R = a \left[\left(\frac{\partial R}{\partial P} \right)_1 \Delta P + \left(\frac{\partial R}{\partial E_0} \right)_1 \Delta E_0 + P_2 \Delta \left(\frac{\partial R}{\partial P} \right) + E_{0,2} \Delta \left(\frac{\partial R}{\partial E_0} \right) \right] \quad (9)$$

$$213 \quad + (1-a) \left[\left(\frac{\partial R}{\partial P} \right)_2 \Delta P + \left(\frac{\partial R}{\partial E_0} \right)_2 \Delta E_0 + P_1 \Delta \left(\frac{\partial R}{\partial P} \right) + E_{0,1} \Delta \left(\frac{\partial R}{\partial E_0} \right) \right]$$

213 where the subscript 1 and 2 denotes the reference and the evaluation periods, respectively. a is a
 214 weighting factor and varies from 0 to 1. As suggested by Zhou *et al.* (2016), I set $a = 0.5$. Equation (9)
 215 thus gave an estimation of ΔR_P , ΔR_{E_0} , and ΔR_n as follows:

$$216 \quad \Delta R_P = 0.5 \Delta P \left[\left(\frac{\partial R}{\partial P} \right)_1 + \left(\frac{\partial R}{\partial P} \right)_2 \right] \quad (10a)$$

$$217 \quad \Delta R_{E_0} = 0.5 \Delta E_0 \left[\left(\frac{\partial R}{\partial E_0} \right)_1 + \left(\frac{\partial R}{\partial E_0} \right)_2 \right] \quad (10b)$$

$$218 \quad \Delta R_n = 0.5 \Delta \left(\frac{\partial R}{\partial P} \right) (P_1 + P_2) + 0.5 \Delta \left(\frac{\partial R}{\partial E_0} \right) (E_{0,1} + E_{0,2}) \quad (10c)$$

219 2.5 Data

220 I collected data of runoff and climate of 21 selected catchments from previous studies (Table 1).
 221 The change-point years gave in the studies was directly used to determine the reference and evaluation
 222 periods for the LI method. As mentioned above, the LI method further divides the evaluation period into
 223 a number of subperiods. For the sake of comparison, the last subperiod of the evaluation period was
 224 used as the evaluation period for the decomposition, the total differential and the complementary
 225 methods (It can be equally considered that all of the four methods used the last subperiod as the
 226 evaluation period, but the LI method cares about the intermediate period between the reference and the
 227 evaluation periods and the others do not). Nine of the 21 catchments had a reference period comprising
 228 only one subperiod (Table 1), and the others had two to seven.

229 The 21 selected catchments were located in diverse climates and landscapes. Among them, 14
 230 are from Australia and 7 from China (Table 1). The catchments spanned from tropical to subtropical and
 231 temperate and from humid to semi-humid and semi-arid regions, with mean annual rainfall varying
 232 from 506 to 1014 mm and potential evaporation from 768 to 1169 mm. The index of dryness ranges
 233 between 0.86 and 1.91. The catchment areas vary by five orders of magnitude from 1.95 to 121,972
 234 with a median 606 km². The key data includes annual runoff, precipitation, and potential evaporation.
 235 The record length varied between 15 and 75 with a median of 35 years. Among the 21 catchments, the
 236 changes from the reference to the evaluation period ranged between -271 and 79 mm yr⁻¹ for
 237 precipitation, and -35 and 41 mm yr⁻¹ for potential evaporation (Table 2). The coeval change in the
 238 parameter n of the MCY equation ranged between -0.2 to 2.53. All of the catchments experienced both
 239 climate change and land cover change over the observation period. The mean annual streamflow
 240 reduced for all of them, by from 0.43 to 229 with a median 38 mm yr⁻¹. More details of data and the
 241 catchments can be found in Zhang *et al.* (2011), Sun *et al.* (2014), Zhang *et al.* (2010), Zheng *et al.*
 242 (2009), Jiang *et al.* (2015), and Gao *et al.* (2016).



243

244 3 Results

245 3.1 Comparisons with other methods

246 The LI method first partitions the whole observation period into the reference and evaluation
247 periods, then further divides the latter into a number of subperiods and evaluates the contributions to
248 runoff from climate and catchment changes for each subperiod, and finally adds up the derived
249 contributions. Table 3 lists all of the resultant values of ΔR_P , ΔR_{E_0} , and ΔR_n of the LI method, together
250 with the three other methods.

251 Fig. 2(a) compares the resultant ΔR_n of the LI method and the decomposition method. Although
252 they are quite similar, the discrepancies between them can be up to $>20 \text{ mm yr}^{-1}$. The decomposition
253 method assumes that climate change occurs first and then human interferences cause a sudden change in
254 catchment properties. Such a fictitious path is identical to the broken line AB+BC in Fig. 1, provided
255 that x represents climate factors and y catchment properties. As a result, the decomposition method can
256 be considered as a special case of the LI method when adopting the broken line AB+BC as the integral
257 path, as was demonstrated clearly in Fig. 2(b).

258 The total differentiae method is predicated on an approximate equation, *i.e.* Eq. (7). The LI
259 method reveals that the precise form of the equation is $\Delta R = \overline{\lambda_P} \Delta P + \overline{\lambda_{E_0}} \Delta E_0 + \overline{\lambda_n} \Delta n$ (*i.e.* Eq. (D2) in
260 Appendix D), where $\overline{\lambda_P}$, $\overline{\lambda_{E_0}}$ and $\overline{\lambda_n}$ (Table 4) denote the path-averaged sensitivity of R to P , E_0 , and n ,
261 respectively. All points along the path have the same weight in determining $\overline{\lambda_P}$, $\overline{\lambda_{E_0}}$ and $\overline{\lambda_n}$. To
262 determine them, the total differential method utilizes only the initial state and the complementary
263 method utilizes the initial and the terminal states. Neglecting the intermediate states between the initial
264 and the terminal ones even possibly results in a reverse trend estimation (see ΔR_{E_0} for Catchment NO. 1
265 in Table 3). Although the elasticity method exploits information contained over the entire observation
266 period (e.g. Zheng *et al.*, 2009; Wang *et al.*, 2013), the resultant descriptive statistics of climate
267 elasticity may not be robust (Roderick and Farquhar, 2011; Liang *et al.*, 2015).

268 Superior to the total differential method, the sum of ΔR_P , ΔR_{E_0} , and ΔR_n always equaled to ΔR
269 for the LI method. In addition, examination of the subperiods of the evaluation period revealed that
270 $\partial R / \partial n$ was more temporally variable than $\partial R / \partial P$ and $\partial R / \partial E_0$ (discussed below). For this reason, ΔR_n
271 showed considerable discrepancies between the two methods although ΔR_P as well as ΔR_{E_0} was highly
272 correlated.

273 As with the LI method, the complementary method produced a ΔR on a par with the observed
274 values. The ΔR_P , ΔR_{E_0} , and ΔR_n estimated by the complementary method were all in good agreement
275 with the LI method (Fig. 4). However, the LI method often yielded values beyond the bounds given by
276 the complementary method (Fig. 5); this is because the initial and terminal states are not equivalent to
277 the maximum and minimum values over the integral path.



278 3.2 The spatio-temporal variability of the path-averaged sensitivities

279 $\overline{\lambda}_P$, $\overline{\lambda}_{E_0}$ and $\overline{\lambda}_n$ implies the average runoff change induced by a unit change in P , E_0 and n ,
280 respectively (Appendix D). Their spatio-temporal variability is relevant to the prediction of the runoff
281 change. To evaluate their temporal variability, I calculated $\overline{\lambda}_P$, $\overline{\lambda}_{E_0}$ and $\overline{\lambda}_n$ for each subperiod of the
282 evaluation period and assessed their deviation from those for the whole evaluation period. As shown in
283 Fig. 6, the deviation was rather limited for $\overline{\lambda}_P$ (averaged 8.6%) and $\overline{\lambda}_{E_0}$ (averaged 13%), but was
284 considerable for $\overline{\lambda}_n$ (averaged 41%). Hence, it seems quite safe to predict the future climate effects on
285 runoff using earlier $\overline{\lambda}_P$ and $\overline{\lambda}_{E_0}$, but care must be taken when using earlier $\overline{\lambda}_n$ to predict future
286 catchment effect on runoff.

287 Different from the temporal variability, $\overline{\lambda}_P$, $\overline{\lambda}_{E_0}$ and $\overline{\lambda}_n$ all varied greatly, by up to several or
288 even ten folds, between the studied catchments (Table 4). It was found that there were good correlations
289 between $\overline{\lambda}_P$ and P , between $\overline{\lambda}_{E_0}$ and P , and between $\overline{\lambda}_n$ and n (Fig. 7). Fig. 8 shows that Eq. (2)
290 reproduced $\overline{\lambda}_P$, $\overline{\lambda}_{E_0}$ and $\overline{\lambda}_n$ very well taking the long-term means of P , E_0 , and n as inputs, a fact that the
291 dependent variable approached its average if setting the independent variables to be their averages. The
292 finding would greatly facilitate the prediction of future climate effect on runoff as $\overline{\lambda}_P$ and $\overline{\lambda}_{E_0}$ was
293 rather stable over time as previously mentioned.

294 Runoff data and in turn, the parameter n in the MCY equation, are often unavailable. It is thus
295 desirable to make predictions of $\overline{\lambda}_P$, $\overline{\lambda}_{E_0}$ and $\overline{\lambda}_n$ in the absence of the parameter n . I developed three
296 strategies as follows: 1) using Eq. (2) and assuming $n = 2$ as n is typically in a small range from 1.5 to
297 2.6 (Roderick and Farquhar, 2011); 2) using P and E_0 to establish regression models; 3) using the aridity
298 index to establish regressions as it appeared to be more correlated with both $\overline{\lambda}_P$ and $\overline{\lambda}_{E_0}$ than P and E_0
299 (Fig. 7). As shown in Fig. 9, the three strategies have similar performance although the second one
300 seems to perform better. All of the strategies gave acceptable predictions of $\overline{\lambda}_P$ and $\overline{\lambda}_{E_0}$, but rather poor
301 results for $\overline{\lambda}_n$ as it was primarily controlled by n (Fig. 7). It was thus needed to seek more sophisticated
302 approaches to predict the future catchment effect on runoff in the absence of runoff observations.
303

304 4 Discussion

305 The LI method re-defines the widely-used concept of sensitivity at a point as the path-averaged
306 sensitivity. The method highlights the role of the evolutionary path in determining the resultant partition.
307 Yet, it seems that no studies have taken into account the path issue when evaluating the relative
308 influences of drivers. It has been a great concern for hydrologist, agricultural scientist, geoscientist,
309 catchment managers and others for more than 50 years that how much runoff change a 10% or 20%
310 change in precipitation would result in (Roderick and Farquhar, 2011; Yang *et al.*, 2014). The LI
311 method reveals that the answer to the question varies with both the timing and magnitude of the
312 precipitation change, not on the magnitude alone. Berghuijs and Woods (2016) claimed an asymmetry
313 between spatial and temporal partitioning of precipitation into streamflow and evaporation.
314 Unfortunately, they did not take account of the difference between the evolutionary paths over space
315 and time, which also play a role in determining the resultant partitioning.



316 Mathematically, the LI method is unrelated to a functional form and applies to communities
317 other than just hydrology. For example, identifying the carbon emission budgets (an allowable
318 amount of anthropogenic CO₂ emission consistent with a limiting warming target), is crucial for global
319 efforts to mitigate climate change. The LI method suggested that the emission budgets depends on both
320 the emission magnitude and pathway (timing of emissions), in line with a recent study by Gasser *et al.*
321 (2018), and an optimal pathway would bring about an elevated carbon budget unless the carbon-climate
322 system behaves in a linear fashion. The LI method applies equally to the case of spatial series of data.
323 Given a model that relates fluvial or aeolian sediment load to the influencing factors, for example, the
324 LI method can be used to separate the contributions of the factors to the sediment-load change along a
325 river or in the along-wind direction

326

327 **5 Conclusions**

328 Based on the line integral, I found a solution to partition the effects of a number of independent
329 variables on the change in the dependent variable. I then applied the method to partition the effects on
330 runoff of climatic and catchment conditions within the Budyko framework. The method reveals that in
331 addition to the change magnitude, the change pathways of climatic and catchment conditions also exert
332 control on their impacts on runoff. Instead of using the runoff sensitivity at a point, the LI method uses
333 the path-averaged sensitivity, thereby ensuring a mathematically precise partition. I further examined
334 the spatiotemporal variability of the path-averaged sensitivity. Time-wise the runoff sensitivity is stable
335 to climate but highly variable to catchment properties, suggesting that it is reliable to predict future
336 climate effects using earlier observations but care must be taken when predicting the catchment effects.
337 Space-wise (between catchments) the runoff sensitivity was highly variable both to climatic and
338 catchment conditions, but it can be well depicted by the long-term means of the climatic and catchment
339 conditions. As a mathematically accurate scheme, the LI method has the potential to be a generic
340 attribution approach in the environmental sciences.

341

342 **Data availability**

343 The data used in this study are freely available by contacting the authors.

344

345 **Author contribution**

346 MZ designed the study, analysing the data and wrote the manuscript.

347

348 **Competing interests**

349 The authors declare that they have no conflict of interest.

350



351 **Appendix A: Derivation of equation** $\Delta z = \int_L f_x(x, y)dx + \int_L f_y(x, y)dy$

352 We define that the curve L in Fig. 1 is given by a parametric equation: $x = x(t)$, $y = y(t)$,
 353 $t \in [t_0, t_N]$, then $\Delta z = z_N - z_0 = f[x(t_N), y(t_N)] - f[x(t_0), y(t_0)]$. Substituting the parametric equations, we
 354 get:

355 The right-hand side of the equation = $\int_{t_0}^{t_N} f_x[x(t), y(t)]dx(t) + \int_{t_0}^{t_N} f_y[x(t), y(t)]dy(t)$
 356 = $\int_{t_0}^{t_N} \{f_x[x(t), y(t)]x'(t) + f_y[x(t), y(t)]y'(t)\} dt$ (A1)

357 Let $g(t) = f[x(t), y(t)]$, and after using the chain rule to differentiate g with respect to t , we obtain:

358 $g'(t) = \frac{\partial g}{\partial x} \frac{dx}{dt} + \frac{\partial g}{\partial y} \frac{dy}{dt} = f_x[x(t), y(t)]x'(t) + f_y[x(t), y(t)]y'(t)$ (A2)

359 It shows that $g'(t)$ is just the integrand in Eq. (A1), Eq. (A1) can then be rewritten as:

360 The right-hand side of the equation = $\int_{t_0}^{t_N} g'(t) dt = [g(t)]_{t_0}^{t_N} = g(t_N) - g(t_0)$
 361 = $f[x(t_N), y(t_N)] - f[x(t_0), y(t_0)]$ = The left-hand side of the equation

362 **Appendix B: The sum of $\int_L f_x(x, y)dx$ and $\int_L f_y(x, y)dy$ is path independent**

363 **Theorem:** Given an open simply-connected region G (i.e., no holes in G) and two functions $P(x, y)$
 364 and $Q(x, y)$ that have continuous first-order derivatives, if and only if $\partial P / \partial y = \partial Q / \partial x$ throughout G ,
 365 then $\int_L P(x, y)dx + \int_L Q(x, y)dy$ is path independent, i.e., it depends solely on the starting and ending
 366 point of L .

367 We have $\partial f_x / \partial y = \partial^2 z / \partial x \partial y$ and $\partial f_y / \partial x = \partial^2 z / \partial y \partial x$. As $\partial^2 z / \partial x \partial y = \partial^2 z / \partial y \partial x$, we can state that
 368 $\partial f_x / \partial y = \partial f_y / \partial x$, meeting the above condition and proving that $\int_L f_x(x, y)dx + \int_L f_y(x, y)dy$ is path
 369 independent. The statement was further exemplified using a fictitious example in Appendix C.

370 **Appendix C. A fictitious example to show how the LI method works**

371 It is assumed that runoff (R , mm yr⁻¹) at a site increases from 120 to 195 mm yr⁻¹ with $\Delta R = 75$ mm
 372 yr⁻¹; meanwhile, precipitation (P , mm yr⁻¹) varies from 600 to 650 mm yr⁻¹ ($\Delta P = 75$ mm yr⁻¹) and
 373 runoff coefficient (C_R , dimensionless) from 0.2 to 0.3 ($\Delta C_R = 0.1$). The goal is to partition ΔR into the
 374 effects of precipitation (ΔR_P) and runoff coefficient (ΔR_{C_R}) provided that P and C_R are independent.
 375 We have a function $R = PC_R$ and its partial derivatives $\partial R / \partial P = C_R$ and $\partial R / \partial C_R = P$. Given a path L
 376 along which P and C_R change and using Eq. (3), the LI method evaluates ΔR_P and ΔR_{C_R} as:

377 $\Delta R_{C_R} = \int_L \partial R / \partial C_R dC_R = \int_L P dC_R$ and $\Delta R_P = \int_L \partial R / \partial P dP = \int_L C_R dP$ (C1)



378 The result differs depending on L but the sum of ΔR_P and ΔR_{C_R} uniformly equals ΔR . It will be
 379 demonstrated using Fig. 1, in which the x -axis represents C_R and the y -axis P . Point A denotes the initial
 380 state ($C_R = 0.2, P = 600$) and point C the terminal state ($C_R = 0.3, P = 650$). I calculated ΔR_P and ΔR_{C_R}
 381 along three fictitious paths as follows:

382 1) $L=AC$. Line segment AC has equation $P = 500C_R + 500, 0.2 \leq C_R \leq 0.3$. Let's take C_R as the
 383 parameter and write the equation in the parametric form as $P = 500C_R + 500, C_R = C_R, 0.2 \leq C_R \leq 0.3$.
 384 By substituting the equation into Eq. (C1), we have:

$$385 \quad \Delta R_{C_R} = \int_{AC} P dC_R = \int_{0.2}^{0.3} (500C_R + 500) dC_R = 62.5$$

$$386 \quad \Delta R_P = \int_{AC} C_R dP = \int_{AC} C_R d(500C_R + 500) = 500 \int_{0.2}^{0.3} C_R dC_R = 12.5$$

387 2) $L=AB+BC$. To evaluate on the broken line, we can evaluate separately on AB and BC and then sum
 388 them up. The equation for AB is $P = 600, 0.2 \leq C_R \leq 0.3$, and is $C_R = 0.3, 600 \leq P \leq 650$ for BC.
 389 Notes that a constant C_R or P implies that $dC_R = 0$ or $dP = 0$. Eq. (C1) then becomes:

$$390 \quad \Delta R_{C_R} = \int_{AB+BC} P dC_R = \int_{AB} P dC_R + \int_{BC} P dC_R = \int_{0.2}^{0.3} 600 dC_R + 0 = 60$$

$$391 \quad \Delta R_P = \int_{AB+BC} C_R dP = \int_{AB} C_R dP + \int_{BC} C_R dP = 0 + \int_{600}^{650} 0.3 dP = 15$$

392 3) $L=AD+DC$. The equation for AD is $C_R = 0.2, 600 \leq P \leq 650$ and is $P = 650, 0.2 \leq C_R \leq 0.3$ for
 393 DC. ΔR_P and ΔR_{C_R} are evaluated as:

$$394 \quad \Delta R_{C_R} = \int_{AD+DC} P dC_R = \int_{AD} P dC_R + \int_{DC} P dC_R = 0 + \int_{0.2}^{0.3} 650 dC_R = 65$$

$$395 \quad \Delta R_P = \int_{AD+DC} C_R dP = \int_{AD} C_R dP + \int_{DC} C_R dP = \int_{600}^{650} 0.2 dP + 0 = 10$$

396 As we expected, the sum of ΔR_P and ΔR_{C_R} persistently equals ΔR although ΔR_P and ΔR_{C_R} varies with
 397 L .
 398

399 **Appendix D: Derivation of $\Delta R = \overline{\lambda_P} \Delta P + \overline{\lambda_{E_0}} \Delta E_0 + \overline{\lambda_n} \Delta n$**

400 If we partition the interval $[x_0, x_N]$ in Fig. 1 into N distinct bins of the same width $\Delta x_i = \Delta x/N$. Eq.
 401 (3a) can then be rewritten as:

$$402 \quad \Delta Z_x = \int_L f_x(x, y) dx = \lim_{\tau \rightarrow 0} \sum_{i=0}^{N-1} f_x(x_i, y_i) \Delta x_i = \lim_{N \rightarrow \infty} N \Delta x_i \frac{\sum_{i=0}^{N-1} f_x(x_i, y_i)}{N} = \Delta x \lim_{N \rightarrow \infty} \frac{\sum_{i=0}^{N-1} f_x(x_i, y_i)}{N} = \overline{\lambda_x} \Delta x$$

403 where $\overline{\lambda_x} = \lim_{N \rightarrow \infty} \frac{\sum_{i=0}^{N-1} f_x(x_i, y_i)}{N}$, denoting the average of $f_x(x, y)$ along the curve L . Likewise, we have

404 $\Delta Z_y = \overline{\lambda_y} \Delta y$, where $\overline{\lambda_y}$ denotes the average of $f_y(x, y)$ along the curve L . As a result, we have:

$$405 \quad \Delta Z = \overline{\lambda_x} \Delta x + \overline{\lambda_y} \Delta y \quad (D1)$$



406 The result can readily be extended to a function of three variables. Applying the mathematic
407 derivation above to the MCY Equation results in a precise form of Eq. (7):

$$408 \Delta R = \Delta R_P + \Delta R_{E_0} + \Delta R_n = \overline{\lambda_P} \Delta P + \overline{\lambda_{E_0}} \Delta E_0 + \overline{\lambda_n} \Delta n, \quad (D2)$$

409 where $\Delta R_P = \overline{\lambda_P} \Delta P$, $\Delta R_{E_0} = \overline{\lambda_{E_0}} \Delta E_0$, $\Delta R_n = \overline{\lambda_n} \Delta n$, and $\overline{\lambda_P}$, $\overline{\lambda_{E_0}}$ and $\overline{\lambda_n}$ denote the arithmetic mean of $\partial R / \partial P$,
410 $\partial R / \partial E_0$, and $\partial R / \partial n$ along a path of climate and catchment changes, respectively. Because $\overline{\lambda_P} = \Delta R_P / \Delta P$,
411 $\overline{\lambda_{E_0}} = \Delta R_{E_0} / \Delta E_0$, and $\overline{\lambda_n} = \Delta R_n / \Delta n$, $\overline{\lambda_P}$, $\overline{\lambda_{E_0}}$ and $\overline{\lambda_n}$ also implies the runoff change due to a unit change in
412 P , E_0 and n , respectively.
413

414 Acknowledgments

415 This work was funded by the National Natural Science Foundation of China (41671278), the GDAS'
416 Project of Science and Technology Development (2019GDASYL-0103043) and (2019GDASYL-
417 0502004). I thank Mr. Y.Q. Zheng for his assistance with the mathematic derivations.
418

419 References

- 420 Barnett, T. P., Pierce, D. W., Hidalgo, H. G., Bonfils, C., Santer, B. D., Das, T., Bala G., Woods, A. W.,
421 Nozawa, T., Mirin, A. A., Cayan D. R., and M. D. Dettinger: Human-induced changes in the
422 hydrology of the western United States. *Science*, 319(5866), 1080-1083.
423 <https://doi.org/10.1126/science.1152538>, 2008.
- 424 Berghuijs, W. R., R. A. Woods: Correspondence: Space-time asymmetry undermines water yield
425 assessment. *Nature Communications* 7, 11603. <https://doi.org/10.1038/ncomms11603>, 2016.
- 426 Binley, A. M., Beven, K. J., Calver, A., and L. G. Watts: Changing responses in hydrology: assessing
427 the uncertainty in physically based model predictions. *Water Resources Research*, 27(6), 1253-1261.
428 <https://doi.org/10.1029/91WR00130>, 1991.
- 429 Brown, A. E., Zhang, L., McMahon, T. A., Western, A. W. and R. A. Vertessy: A review of paired
430 catchment studies for determining changes in water yield resulting from alterations in vegetation.
431 *Journal of Hydrology* 310, 26–61. <https://doi.org/10.1016/j.jhydrol.2004.12.010>, 2005.
- 432 Budyko, M. I.: *Climate and Life*. Academic, N. Y. 1974.
- 433 Choudhury, B. J.: Evaluation of an empirical equation for annual evaporation using field observations
434 and results from a biophysical model. *Journal of Hydrology*, 216, 99–110.
435 [https://doi.org/10.1016/S0022-1694\(98\)00293-5](https://doi.org/10.1016/S0022-1694(98)00293-5), 1999.
- 436 Dey, P., and A. Mishra: Separating the impacts of climate change and human activities on streamflow:
437 A review of methodologies and critical assumptions. *Journal of Hydrology*, 548, 278-290.
438 <https://doi.org/10.1016/j.jhydrol.2017.03.014>, 2017.
- 439 Gao, G., Ma, Y., and B. Fu: Multi-temporal scale changes of streamflow and sediment load in a loess
440 hilly watershed of China. *Hydrological Processes*, 30(3), 365-382, 10.1002/hyp.10585, 2016.
- 441 Gasser, T., M. Kechiar, P. Ciais, E. J. Burke, T. Kleinen, D. Zhu, Y. Huang, A. Ekici, and M.
442 Obersteiner: Path-dependent reductions in CO₂ emission budgets caused by permafrost carbon
443 release. *Nature Geoscience*, 11, 830–835. <https://doi.org/10.1038/s41561-018-0227-0>, 2018.



- 444 Jiang, C., Xiong, L., Wang, D., Liu, P., Guo, S., and Xu C.: Separating the impacts of climate change
445 and human activities on runoff using the Budyko-type equations with time-varying parameters.
446 *Journal of Hydrology*, 522, 326-338, 10.1016/j.jhydrol.2014.12.060, 2015.
- 447 Liang, W., D. Bai, F. Wang, B. Fu, J. Yan, S. Wang, Y. Yang, D. Long, and M. Feng: Quantifying the
448 impacts of climate change and ecological restoration on streamflow changes based on a Budyko
449 hydrological model in China's Loess Plateau. *Water Resources Research*, 51, 6500–6519.
450 <https://doi.org/10.1002/2014WR016589>, 2015.
- 451 Mezentsev, V. S.: More on the calculation of average total evaporation. *Meteorol. Gidrol.*, 5, 24–26,
452 1955.
- 453 Roderick, M. L., and G. D. Farquhar: A simple framework for relating variations in runoff to variations
454 in climatic conditions and catchment properties. *Water Resources Research*, 47, W00G07,
455 <https://doi.org/10.1029/2010WR009826>, 2011.
- 456 Sankarasubramanian, A., R. M. Vogel, and J. F. Limbrunner: Climate elasticity of streamflow in the
457 United States. *Water Resources Research*, 37(6), 1771-1781.
458 <https://doi.org/10.1029/2000WR900330>, 2001.
- 459 Schaake, J. C.: From climate to flow. *Climate Change and U.S. Water Resources*, edited by P. E.
460 Waggoner, chap. 8, pp. 177 - 206, John Wiley, N. Y. 1990.
- 461 Sposito, G.: Understanding the Budyko equation. *Water*, 9(4), 236. <https://doi.org/10.3390/w9040236>,
462 2017.
- 463 Sun, Y., Tian, F., Yang, L., and H. Hu: Exploring the spatial variability of contributions from climate
464 variation and change in catchment properties to streamflow decrease in a mesoscale basin by three
465 different methods. *Journal of Hydrology*, 508(2), 170-180,
466 <https://doi.org/10.1016/j.jhydrol.2013.11.004>, 2014.
- 467 Wang, D., and M. Hejazi: Quantifying the relative contribution of the climate and direct human impacts
468 on mean annual streamflow in the contiguous United States. *Water Resources Research*, 47, W00J12,
469 <https://doi.org/10.1029/2010WR010283>, 2011.
- 470 Wang, W., Q. Shao, T. Yang, S. Peng, W. Xing, F. Sun, and Y. Luo: Quantitative assessment of the
471 impact of climate variability and human activities on runoff changes: A case study in four
472 catchments of the Haihe River basin, China. *Hydrological Processes*, 27(8), 1158–1174.
473 <https://doi.org/10.1002/hyp.9299>, 2013.
- 474 Xu, X., Yang, D., Yang, H. and Lei, H.: Attribution analysis based on the Budyko hypothesis for
475 detecting the dominant cause of runoff decline in Haihe basin. *Journal of Hydrology*, 510: 530-540.
476 <http://dx.doi.org/10.1016/j.jhydrol.2013.12.052>, 2014.
- 477 Yang, H., D. Yang, Z. Lei, and F. Sun: New analytical derivation of the mean annual water-energy
478 balance equation. *Water Resources Research*, 44, W03410. <https://doi.org/10.1029/2007WR006135>,
479 2008.
- 480 Yang, H., and D. Yang: Derivation of climate elasticity of runoff to assess the effects of climate change
481 on annual runoff. *Water Resources Research*, 47, W07526. <https://doi.org/10.1029/2010WR009287>,
482 2011.
- 483 Yang, H., D. Yang, and Q. Hu: An error analysis of the Budyko hypothesis for assessing the
484 contribution of climate change to runoff. *Water Resources Research*, 50, 9620–9629.
485 <https://doi.org/10.1002/2014WR015451>, 2014.



- 486 Zhang, S., H. Yang, D. Yang, and A. W. Jayawardena: Quantifying the effect of vegetation change on
487 the regional water balance within the Budyko framework. *Geophysical Research Letters*, 43, 1140–
488 1148. <https://doi.org/10.1002/2015GL066952>, 2016.
- 489 Zhang, L., Dawes, W. R. and G. R. Walker: Response of mean annual evapotranspiration to vegetation
490 changes at catchment scale. *Water Resources Research* 37, 701–708. doi; 10.1029/2000WR900325,
491 2001.
- 492 Zhang, L., F. Zhao, A. Brown, Y. Chen, A. Davidson, and R. Dixon: Estimating Impact of Plantation
493 Expansions on Streamflow Regime and Water Allocation. CSIRO Water for a Healthy Country,
494 Canberra, Australia. 2010.
- 495 Zhang, L., F. Zhao, Y. Chen, and R. N. M. Dixon: Estimating effects of plantation expansion and
496 climate variability on streamflow for catchments in Australia. *Water Resources Research*, 47,
497 W12539, <https://doi.org/10.1029/2011WR010711>, 2011.
- 498 Zheng, H., L. Zhang, R. Zhu, C. Liu, Y. Sato, and Y. Fukushima: Responses of streamflow to climate
499 and land surface change in the headwaters of the Yellow River Basin. *Water Resources Research*, 45,
500 W00A19. <https://doi.org/10.1029/2007WR006665>, 2009.
- 501 Zhou, S., B. Yu, L. Zhang, Y. Huang, M. Pan, and G. Wang (2016), A new method to partition climate
502 and catchment effect on the mean annual runoff based on the Budyko complementary relationship.
503 *Water Resources Research*, 52, 7163–7177. <https://doi.org/10.1002/2016WR019046>, 2016.
- 504
505
506
507
508
509
510
511
512
513
514
515
516
517
518
519
520
521
522
523
524
525
526
527
528
529



530 **Table 1.** Summary of the long-term hydrometeorological characteristics of the selected catchments^a

Catchment No. ^b	Area (km ²)	<i>R</i>	<i>P</i>	<i>E</i> ₀	<i>n</i>	<i>AI</i>	Reference Period	Evaluation Period	The Last Subperiod
1	391	218	1014	935	3.5	0.92	1933-1955	1956-2008	1998-2008
2	16.64	32.9	634	1087	3.16	1.71	1979-1984	1985-2008	1999-2008
3	559	183	787	780	2.68	0.99	1960-1978	1979-2000	1993-2000
4	606	73	729	998	3.07	1.37	1971-1995	1996-2009	2003-2009
5	760	77.9	689	997	2.66	1.45	1970-1995	1996-2009	2003-2009
6	502	57.2	730	988	3.59	1.35	1974-1995	1996-2008	1996-2008
7	673	431	1013	953	1.34	0.94	1947-1955	1956-2008	1998-2008
8	390	139	840	1021	2.61	1.22	1966-1980	1981-2005	1995-2005
9	1130	20.7	633	1077	3.79	1.7	1972-1982	1983-2007	1997-2007
10	3.2	37.5	631	954	3.49	1.51	1989-1991	1992-2009	1999-2009
11	1.95	111	767	901	3.06	1.18	1990-1992	1993-2005	1993-2005
12	89	272	963	826	2.82	0.86	1958-1965	1966-1999	1987-1999
13	243	38.5	735	1010	4.27	1.37	1989-1995	1996-2007	1996-2007
14	56.35	65.8	744	1007	3.35	1.35	1989-1995	1996-2008	1996-2008
15	14484	385	893	1022	1.11	1.14	1970-1989	1990-2000	1990-2000
16	38625	461	985	1087	1.03	1.1	1970-1989	1990-2000	1990-2000
17	59115	388	897	1161	1.02	1.29	1970-1989	1990-2000	1990-2000
18	95217	371	881	1169	1.03	1.33	1970-1989	1990-2000	1990-2000
19	121,972	171	507	768	1.17	1.52	1960-1990	1991-2000	1991-2000
20	106,500	60.5	535	905	2.25	1.69	1960-1970	1971-2009	1999-2009
21	5891	34.4	506	964	2.54	1.91	1952-1996	1997-2011	2004-2011

531 ^a*R*, *P*, and *E*₀ represents mean annual runoff, precipitation and potential evaporation, all in mm yr⁻¹. *n*
 532 (dimensionless) is the parameter representing catchment properties in the MCY equation. *AI* is
 533 dimensionless aridity index ($AI = E_0/P$). Data of Catchments 1-14 were derived from Zhang *et al.*
 534 (2010). Data of Catchments 15-18 were from Sun *et al.* (2014). Data of Catchments 19-21 were from
 535 Zheng *et al.* (2009), Jiang *et al.* (2015), and Gao *et al.* (2016), respectively. I used the change points
 536 given in the literatures to divide the observation period into the reference and elevation periods. The LI
 537 method further divides the evaluation period into a number of subperiods. The column “The Last
 538 Subperiod” denotes the last one, which was used as the evaluation period for the total differential
 539 method, the decomposition method and the complementary method. The bold and italic rows denote
 540 that the column “Evaluation Period” is the same as the column “The Last Subperiod”.

541 ^bCatchments 1-14 are in Australia and the others in China. 1: Adjungbilly CK; 2: Batalling Ck; 3:
 542 Bombala River; 4: Crawford River; 5: Darlot Ck; 6: Eumeralla River; 7: Goobarragandra CK; 8:
 543 Jingellic CK; 9: Mosquito CK; 10: Pine Ck; 11: Red Hill; 12: Traralgon Ck; 13: Upper Denmark River;
 544 14: Yate Flat Ck; 15: Yangxian station, Hang River; 16: Ankang station, Hang River; 17: Baihe station,
 545 Hang River; 18: Danjiangkou station, Hang River; 19: Headwaters of the Yellow River Basin; 20: Wei
 546 River; 21: Yan River.

547
 548
 549
 550
 551



552
 553
 554
 555

Table 2. Comparisons of R (mm yr^{-1}), P (mm yr^{-1}), E_0 (mm yr^{-1}), and n (dimensionless) between the reference and the evaluation periods^a

Catchment No.	R_1	R_2	P_1	P_2	E_{01}	E_{02}	n_1	n_2	ΔR	ΔP	ΔE_0	Δn
1	223	216	959	1038	950	928	2.7	4.1	-7.2	79.2	-21	1.4
2	40.6	31	655	629	1087	1087	3	3.2	-9.7	-27	0	0.2
3	249	127	847	736	780	780	2.3	3.2	-122	-112	0.4	0.9
4	90.6	41.5	753	685	1002	989	2.9	3.7	-49	-67	-13	0.8
5	94.9	46.3	718	633	1000	992	2.5	3	-49	-85	-9	0.5
6	70.8	34.3	756	687	989	987	3.4	4.1	-36	-69	-2	0.6
7	575	406	1123	995	931	957	1.1	1.4	-169	-128	25	0.3
8	139	139	871	821	1043	1008	2.7	2.5	-0.4	-50	-35	0
9	24.1	19.2	659	621	1100	1067	3.7	3.8	-4.9	-37	-33	0.1
10	116	24.3	588	638	927	958	1.7	4.2	-92	50.4	31	2.5
11	297	68	986	716	884	905	2.3	3.6	-229	-271	22	1.3
12	301	265	992	956	820	828	2.7	2.8	-36	-36	7.4	0.1
13	48.5	32.6	752	725	991	1021	4.2	4.4	-16	-28	30	0.2
14	90.4	52.6	753	739	991	1015	2.9	3.7	-38	-14	24	0.8
15	435	295	948	795	1008	1047	1.1	1.2	-139	-153	38	0.1
16	520	353	1035	894	1074	1109	1	1.2	-167	-141	35	0.2
17	441	291	939	820	1149	1182	1	1.2	-151	-119	33	0.2
18	412	296	913	821	1163	1179	1	1.1	-116	-92	15	0.2
19	180	144	512	491	774	751	1.1	1.3	-36	-21	-23	0.2
20	90.2	52.1	585	520	895	908	2.1	2.3	-38	-65	13	0.2
21	37.7	24.6	521	462	954	995	2.6	2.5	-13	-59	41	0

556 ^aThe subscript "1" denotes the reference period and "2" denotes the evaluation period. $\Delta X = X_2 - X_1$ (X as
 557 a substitute for R , P , E_0 , and n).

558
 559
 560
 561
 562
 563
 564
 565
 566
 567
 568
 569
 570
 571
 572
 573



574
 575
 576

Table 3. Effects of precipitation (ΔR_P , mm yr⁻¹), potential evapotranspiration (ΔR_{E_0} , mm yr⁻¹), and catchment (ΔR_n , mm yr⁻¹) changes on the mean annual runoff resulting from the four methods

Catchment NO. ^a	LI Method			Decomposition Method	Total Differential Method			Complementary Method		
	ΔR_P	ΔR_{E_0}	ΔR_n	ΔR_n	ΔR_P	ΔR_{E_0}	ΔR_n	ΔR_P	ΔR_{E_0}	ΔR_n
1	-70.9	-8.99	-24.3	-44.6	-67	4.82	-62	-60.7	4.34	-47.3
2	-6.49	0.95	-9.74	-9.65	-7.2	1.3	-13	-6.23	1.13	-10.2
3	-89	25.9	-140	-128	-104	26.6	-483	-88	25.7	-140
4	-18.1	2.09	-35.4	-36.3	-18	2.37	-58	-14.8	1.99	-38.5
5	-27.9	1.14	-21.3	-18.6	-34	1.18	-27	-28.1	0.97	-20.9
6	-19.9	0.29	-16.7	-14.9	-24	0.36	-22	-19.9	0.29	-16.7
7	-211	-7.19	-101	-90.9	-236	-6.9	-134	-211	-6.21	-102
8	-32.2	12.3	-14.4	-12.6	-35	12.6	-15	-32.9	11.9	-13.3
9	-11.8	3.02	-9.96	-8.45	-13	0.85	-20	-8.76	0.56	-10.5
10	19.47	-5.61	-119	-96.5	0.91	-10	-291	0.56	-6.53	-99.1
11	-150	-7.46	-71.8	-60.7	-188	-9.4	-113	-144	-7.04	-78.3
12	-9.88	-3.99	-79.2	-82	-11	-0.5	-154	-10.8	-0.57	-81.6
13	-6.98	-4.36	-4.54	-4.21	-8	-5.1	-5.2	-7	-4.38	-4.51
14	-4.84	-4.42	-28.7	-27.9	-5.6	-5	-37	-4.85	-4.4	-28.6
15	-104	-8.56	-24.8	-23	-110	-9.4	-27	-103	-8.52	-25.1
16	-99.3	-7.99	-58.8	-56	-105	-8.3	-68	-99	-7.92	-59.1
17	-78.8	-6.26	-63.9	-61	-84	-6.5	-76	-78.6	-6.2	-64.2
18	-60.1	-2.79	-53.5	-52	-64	-2.9	-62	-60	-2.77	-53.6
19	-11.9	3.89	-27.6	-27	-12	3.81	-31	-11.9	3.85	-27.5
20	-27.5	-2.46	-18.5	-17	-31	-4.4	-26	-25.5	-3.47	-19.5
21	-10.4	-3.47	-2.11	-3.4	-9.9	-4.8	-4.8	-8.27	-3.86	-3.82

577 ^aThe bold and italic numbers denote that the evaluation period of the catchment comprised a single
 578 subperiod.
 579
 580
 581
 582
 583
 584
 585
 586
 587
 588
 589
 590
 591



592
 593

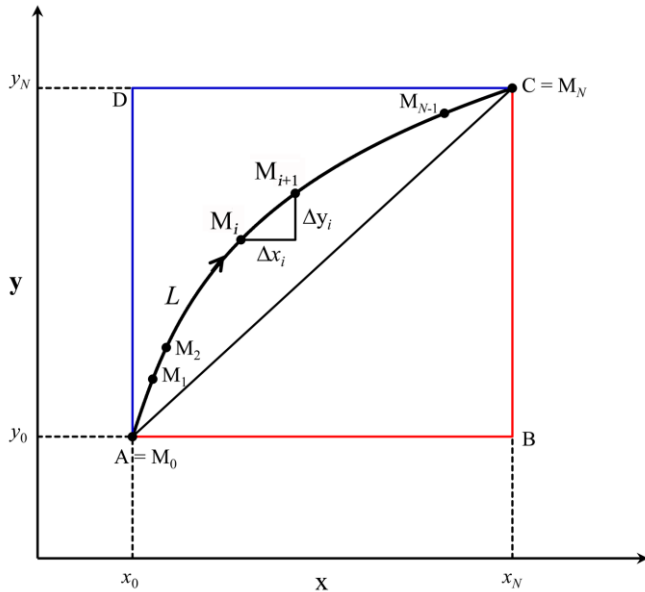
Table 4. Comparisons of the path-averaged with the point sensitivities of runoff^{a, b}

Catchment NO.	$\overline{\lambda_P}$	$\overline{\lambda_{E_0}}$	$\overline{\lambda_n}$	λ_{Pf}	λ_{E_0f}	λ_{nf}	λ_{Pb}	λ_{E_0b}	λ_{nb}
1	0.68	-0.55	-17	0.621	-0.39	-71.8	0.497	-0.32	-39.7
2	0.2	-0.08	-27.3	0.227	-0.1	-30.9	0.168	-0.07	-19.6
3	0.58	-0.36	-26.7	0.68	-0.42	-79	0.473	-0.39	-6.29
4	0.3	-0.16	-30.5	0.39	-0.2	-50.1	0.248	-0.14	-21
5	0.33	-0.14	-43.1	0.394	-0.19	-59.4	0.264	-0.12	-33.2
6	0.29	-0.16	-26.5	0.352	-0.2	-34.9	0.228	-0.12	-19.1
7	0.71	-0.32	-223	0.781	-0.33	-299	0.615	-0.26	-157
8	0.49	-0.26	-77.9	0.478	-0.27	-64.9	0.429	-0.24	-50.7
9	0.16	-0.07	-11.8	0.161	-0.07	-17.6	0.052	-0.02	-4.31
10	0.27	-0.12	-40.9	0.45	-0.16	-99.9	0.101	-0.05	-7.8
11	0.55	-0.35	-56.1	0.695	-0.44	-88.2	0.367	-0.22	-30.7
12	0.72	-0.45	-57.3	0.74	-0.53	-61.1	0.775	-0.67	-16.7
13	0.25	-0.15	-19.8	0.29	-0.17	-22.5	0.219	-0.12	-17.1
14	0.34	-0.18	-37.2	0.393	-0.21	-48.6	0.291	-0.16	-27.8
15	0.68	-0.22	-275	0.719	-0.25	-303	0.635	-0.2	-246
16	0.7	-0.23	-326	0.745	-0.24	-378	0.659	-0.21	-279
17	0.66	-0.19	-320	0.708	-0.2	-378	0.609	-0.18	-267
18	0.65	-0.19	-315	0.692	-0.19	-363	0.614	-0.18	-270
19	0.58	-0.17	-153	0.602	-0.17	-175	0.552	-0.17	-134
20	0.32	-0.12	-50.1	0.402	-0.16	-69.6	0.255	-0.1	-37.7
21	0.2	-0.06	-29.2	0.234	-0.09	-34	0.157	-0.05	-22.6

594 ^a $\overline{\lambda_P}$ (mm mm⁻¹), $\overline{\lambda_{E_0}}$ (mm mm⁻¹), and $\overline{\lambda_n}$ (dimensionless) represent the path-averaged sensitivities of
 595 runoff to precipitation, potential evaporation, and catchment properties. If the evaluation period
 596 comprises only one subperiod, $\overline{\lambda_P}$, $\overline{\lambda_{E_0}}$ and $\overline{\lambda_n}$ was calculated as: $\overline{\lambda_P} = \Delta R_P / \Delta P$, $\overline{\lambda_{E_0}} = \Delta R_{E_0} / \Delta E_0$, and
 597 $\overline{\lambda_n} = \Delta R_n / \Delta n$. If the evaluation period comprises $N > 1$ subperiods, the equations become:
 598 $\overline{\lambda_P} = \sum_{i=1}^N |\Delta R_{Pi}| / \sum_{i=1}^N |\Delta P_i|$, $\overline{\lambda_{E_0}} = - \sum_{i=1}^N |\Delta R_{E_0i}| / \sum_{i=1}^N |\Delta E_{0i}|$, and $\overline{\lambda_n} = - \sum_{i=1}^N |\Delta R_{ni}| / \sum_{i=1}^N |\Delta n_i|$, where the subscript i denotes the i th
 599 subperiod.

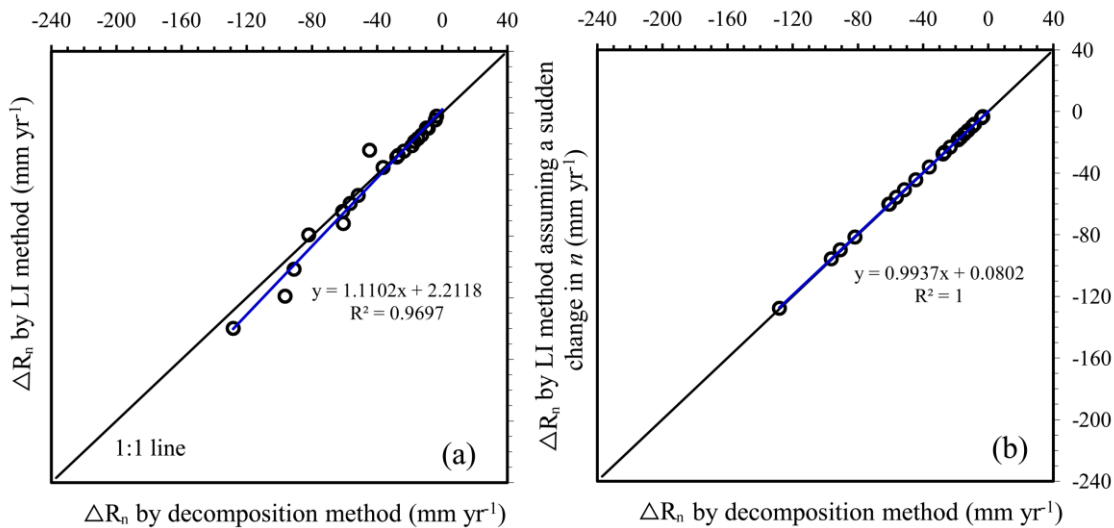
600 ^b λ_P , λ_{E_0} , and λ_n represent the point sensitivities of runoff. The subscript “ f ” represents a forward
 601 approximation, i.e. substituting the observed mean annual values of the reference period into Eq. (2) to
 602 calculate the sensitivities, while the subscript “ b ” represents a backward approximation (Zhou *et al.*,
 603 2016), i.e. substituting the observed mean annual values of the evaluation period into Eq. (2).

604
 605
 606
 607



608
 609
 610

Fig. 1. A schematic plot to illustrate the LI method.

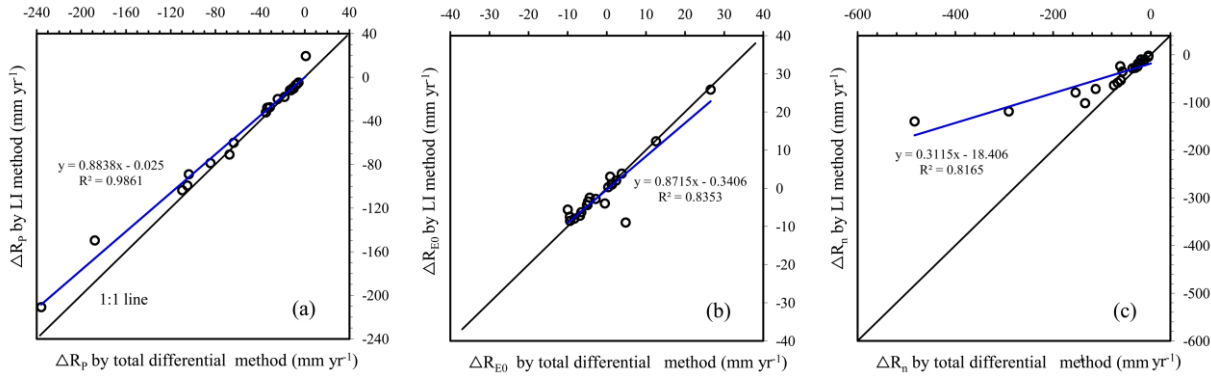


611
 612
 613
 614
 615
 616
 617
 618
 619

Fig. 2. Comparison between the LI method and the decomposition method. (a) Comparison of the estimated contribution to the runoff change from catchment change (ΔR_n); (b) the decomposition method is equivalent to the LI method that assumes a sudden change in catchment properties following climate change. In this case, the integral path of the LI method is the broken line AB+BC in Fig. 1 (x represents climate factors and y catchment properties, *i.e.* n) and $\Delta R_n = \int_{AB+BC} \frac{\partial R}{\partial n} dn = \int_{AB} \frac{\partial R}{\partial n} dn + \int_{BC} \frac{\partial R}{\partial n} dn = 0 + \int_{BC} \frac{\partial R}{\partial n} dn = \int_{n_1}^{n_2} f_n(P_2, E_{02}, n) dn$, where the subscript "1" denotes the reference period and "2" denotes the last subperiod of the evaluation period.

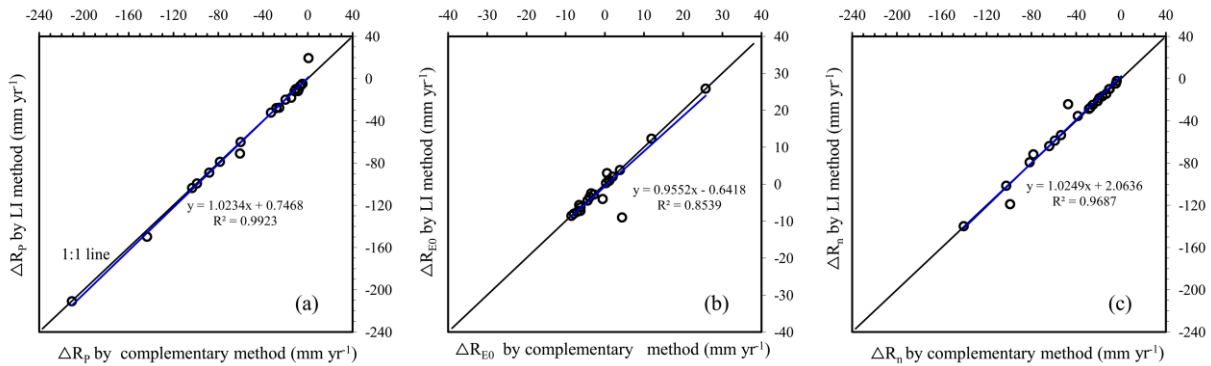


620



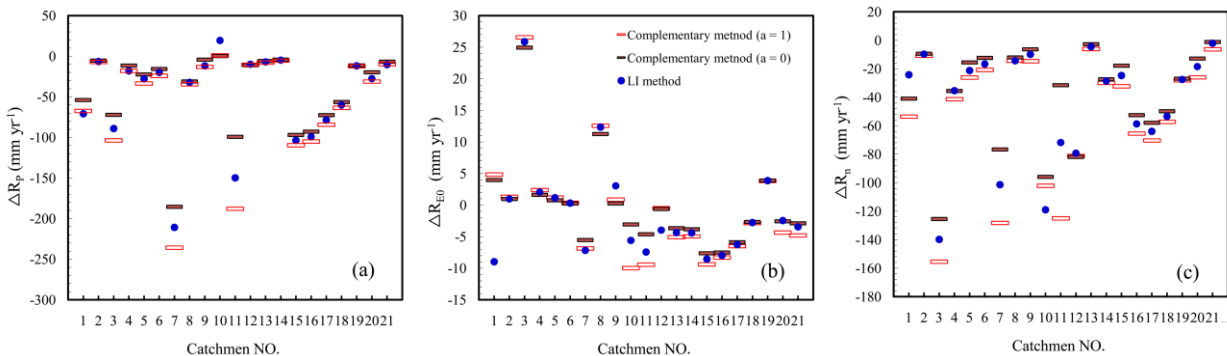
621
 622
 623
 624
 625

Fig. 3. Comparison of the estimated contribution to runoff from the changes in (a) precipitation (ΔR_P), (b) potential evapotranspiration (ΔR_{E_0}), and (c) catchment properties (ΔR_n) between the LI method and the total differential method.



626
 627
 628
 629

Fig. 4. Comparison of (a) ΔR_P , (b) ΔR_{E_0} , and (c) ΔR_n between the LI method and the complementary method ($a = 0.5$).

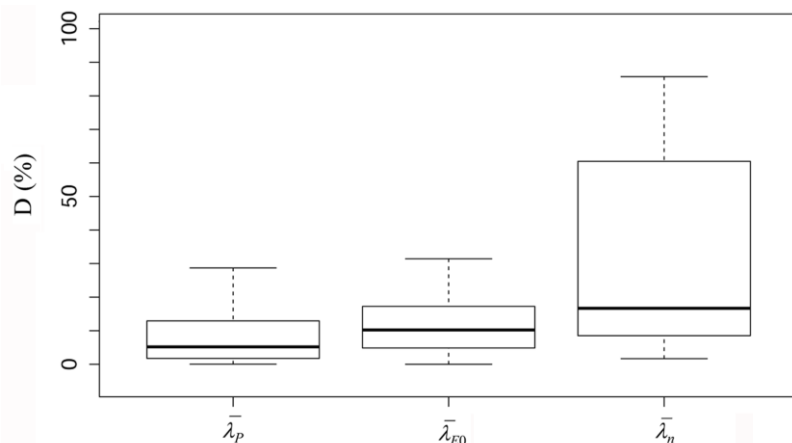


630
 631
 632
 633
 634

Fig. 5. Comparison of (a) ΔR_P , (b) ΔR_{E_0} , and (c) ΔR_n by the LI method with the upper ($a=1$) and lower ($a=0$) bounds given by the complementary method.



635
636

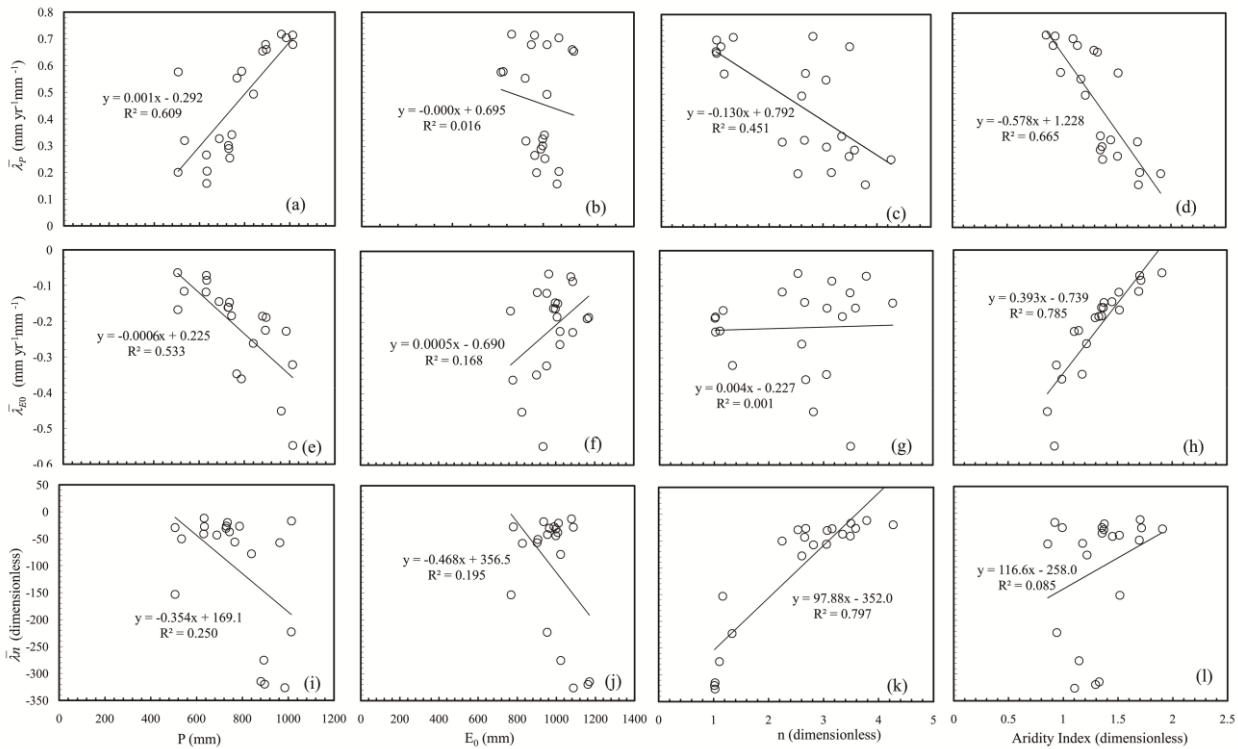


637
638
639
640
641
642
643
644
645
646
647
648
649
650
651
652
653
654
655
656
657
658
659
660
661
662
663
664
665
666
667
668
669

Fig. 6. Boxplots showing the temporal variability of the path-averaged sensitivities of water yield to precipitation ($\bar{\lambda}_P$), potential evapotranspiration ($\bar{\lambda}_{E0}$), and catchment properties ($\bar{\lambda}_n$). D (%) was calculated as the relative difference between the sensitivity of the whole evaluation period and that of a subperiod. In the calculations, I excluded the catchments whose evaluation periods were not long enough to comprise two or more subperiods. Box spans the inter-quartile range (IQR) and solid lines are medians. Whiskers represent data range, excluding statistical outliers, which extend more than 1.5IQR from the box ends.



670



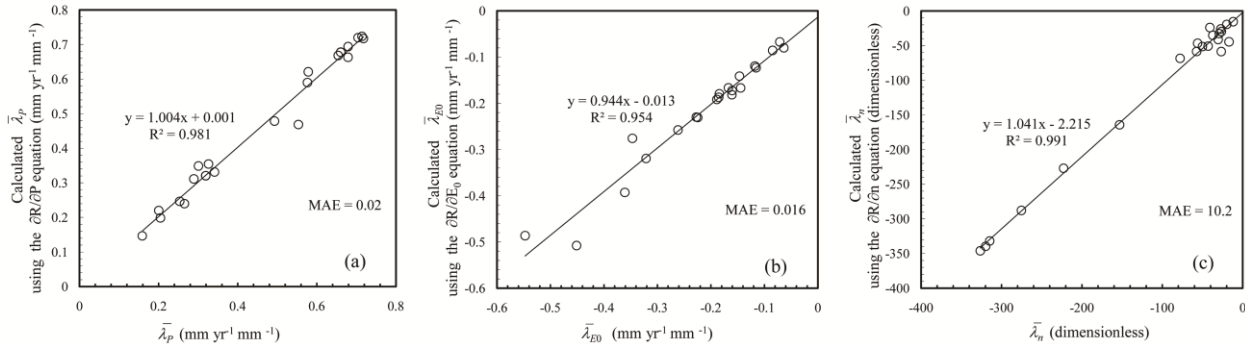
671

Fig. 7. $\bar{\lambda}_P$, $\bar{\lambda}_{E_0}$ and $\bar{\lambda}_n$ in correlation with P , E_0 , n , and aridity index.

672

673

674



675

Fig. 8. Comparisons of $\bar{\lambda}_P$, $\bar{\lambda}_{E_0}$ and $\bar{\lambda}_n$ (given in Table 4) with those predicted using Eq. (2) with the long-term mean values of P , E_0 , and n as inputs. $MAE = N^{-1} \sum_{i=1}^N |O_i - P_i|$, is the mean absolute error,

676

677

678

679

680

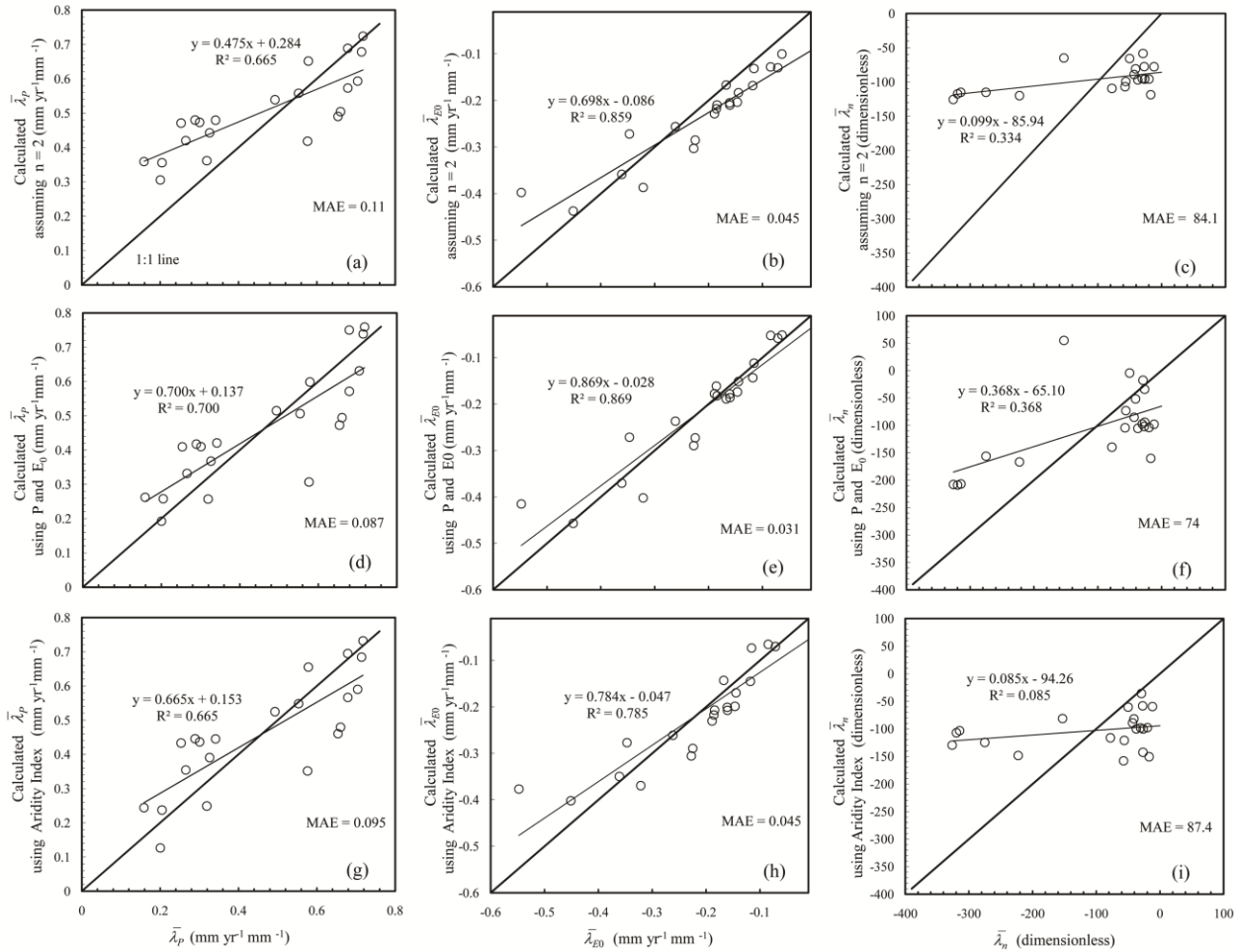
681

682

where O and P are values that actually encountered (given in Table 4) and predicted using Eq. (2) respectively, and N is the number of selected catchments.



683
 684



685
 686
 687
 688
 689
 690
 691

Fig. 9. Comparisons of $\overline{\lambda}_P$, $\overline{\lambda}_{E_0}$ and $\overline{\lambda}_n$ with those predicted by the three strategies. (a)-(c) by Eq. (2) with a constant n ($n = 2$), (d)-(f) by the regression equations established using P and E_0 : $\overline{\lambda}_P = 0.0011P - 0.0006E_0 + 0.21$ ($R^2 = 0.7$), $\overline{\lambda}_{E_0} = 0.0007P - 0.0007E_0 - 0.38$ ($R^2 = 0.87$), and $\overline{\lambda}_n = -0.302P - 0.372E_0 + 493$ ($R^2 = 0.37$), and (g)-(i) by the regression equations established using only the aridity index, as shown in Fig. 7 (d), (h) and (l). MAE was calculated as for Fig. 8.

692
 693
 694